Geophys. J. R. astr. Soc. (1980) **63**, 217–232

A study of large-scale lateral variations of *P* velocity in the upper mantle beneath western Europe

Barbara A. Romanowicz *Institut de Physique du Globe, L.A. 195, 4, Place Jussieu, 75230 Paris, Cedex 05, France*

Received 1980 January 28; in original form 1979 July 23

Summary. A large-scale three-dimensional inversion of teleseismic *P* wave arrival times from ISC bulletins is performed over the part of Europe extending from Scandinavia to the Alps, and down to a depth of 700 km. The inferred velocity variations are compared with those obtained previously for North America in a similar study (Romanowicz 1979).

The models obtained manage to explain one third of the standard deviation in the data, implying that the complicated short wavelength structure in Europe causes substantial scatter that cannot be accounted for by the large-scale model. However, the geographical extent of the large-scale regions of higher and lower velocity anomalies remains stable when the initial specifications of the models are changed, and can therefore be discussed qualitatively in the framework of large-scale tectonic regionalization.

In the uppermost 250 km of the crust and mantle, average velocities are up to 4 per cent higher under the Scandinavian Shield than under the Alps. This is in agreement with previous studies in Europe and may be interpreted primarily in terms of variations of thickness and strength of the low-velocity zone. In this depth range, the average structure for the Hercynian part of western Europe is intermediate between that of the Shield and that of the Alps and Mediterranean region. Velocity fluctuations are not well resolved in the depth range from 250 to 450 km. Between 450 and 700 km, higher velocities are inferred beneath the shield and platform; velocities decrease towards the west and south-west. Under the Alps, velocities appear to be slightly higher than average. The higher velocities under the shield agree with those inferred between depths of 450 and 700 km in the central stable part of North America, suggesting that this may be a general feature of shields and platforms. The relatively higher velocities under the Alps may be compared to the lower velocities obtained beneath the western US, suggesting that the deep structure under major orogenic belts may be related to their mode of formation.

Introduction

A three-dimensional inversion of teleseismic *P* wave arrival times from ISC bulletins over the United States (Romanowicz 1979) has yielded results showing significant lateral variation in

P wave velocity down to a depth of at least 700 km. Moreover, the regionalization determined by the deep heterogeneities was correlated with the surface features in a manner that implied important consequences for the dynamics of the upper mantle beneath that region of the world (Romanowicz & Allègre 1979).

In this paper, we have attempted to apply the same method to western European teleseismic *P* arrival data, in an effort to investigate the large-scale structure at depth under Europe and compare it to the North American results.

A look at the tectonic map of Europe (Schatsky, Bogdanoff & Mouratov 1964) is enough to convince us of the complexity of structure of this part of the world. In particular, the main tectonic features are arranged in a much more contorted pattern at smaller scale than those of the United States, especially in the south, where the presence of plate boundaries complicates the structure of the Mediterranean region (McKenzie 1972; Tapponnier 1977). In spite of fewer studies than on the North American continent, evidence for lateral heterogeneities is abundant. Investigation of the crust by numerous refraction studies (Prodehl 1977) has shown important lateral variations of the depth to the Moho discontinuity in western Europe, and changes in the structure of the crust have been demonstrated to occur over lateral distances of only a few hundred kilometres, as, for example, in France (Souriau 1978). However, for the purpose of this study, three main units may be distinguished: to the north and north-east, a 'stable' region consisting of the Baltic shield and platform defines the first unit. The second unit comprises the western Caledonian and Hercynian areas. Finally the third unit includes the Mesozoic and Cenozoic folded regions of central Europe and the Mediterranean, as shown in Fig. 1, which is adapted from Schatsky *et al.* (1964). Due to a lack of available data as far as upper mantle structure is concerned, most seismological studies have distinguished only two regions: southern and western Europe on the one hand, and the Precambrian shield and platform, on the other. Lateral differences to depths of a few hundred kilometres between these two regions are now widely acknowledged. Studies of *P* station anomalies (Herrin & Taggart 1968; Lilwall & Douglas 1970; Poupinet 1977) have shown systematically earlier arrivals over the Scandinavian shield than in central and southern Europe. Studies of travel times to the Norsar array (England, Worthington & King 1976; England, Kennett & Worthington 1978) favour differences of structure down to depths of at least 300 km between the Scandinavian shield and south-western Europe. Finally, surface wave studies (Knopoff, Mueller & Pilant 1966; Seidl 1971; Sprecher 1976; Nolet 1977; Patton 1978; Panza 1978; Cara, Nercessian & Nolet 1980) find a well-developed mantle low-velocity zone for shear waves in south-western Europe, and particularly under the Alps, while such a zone is much weaker under Scandinavia.

Given a good distribution of stations and events, a three-dimensional inversion of teleseismic *P* arrival data on a large scale permits an investigation of the upper mantle to greater depth, with less horizontal averaging of possible heterogeneities.

In view of the results found for the United States (Romanowicz 1979) and of the data available as will be seen below, we shall be mainly interested in the possible deep differences between the northern shield and platform region and the tectonically younger provinces to the south. The paper on the deep structure under the United States (Romanowicz 1979) will be henceforth referred to as Paper I.

The data

The data used in this study are teleseismic ($30^\circ < \Delta < 100^\circ$) *P* wave arrival times at European stations, as read from the bulletins of the ISC for the 10 yr period 1964–73. The

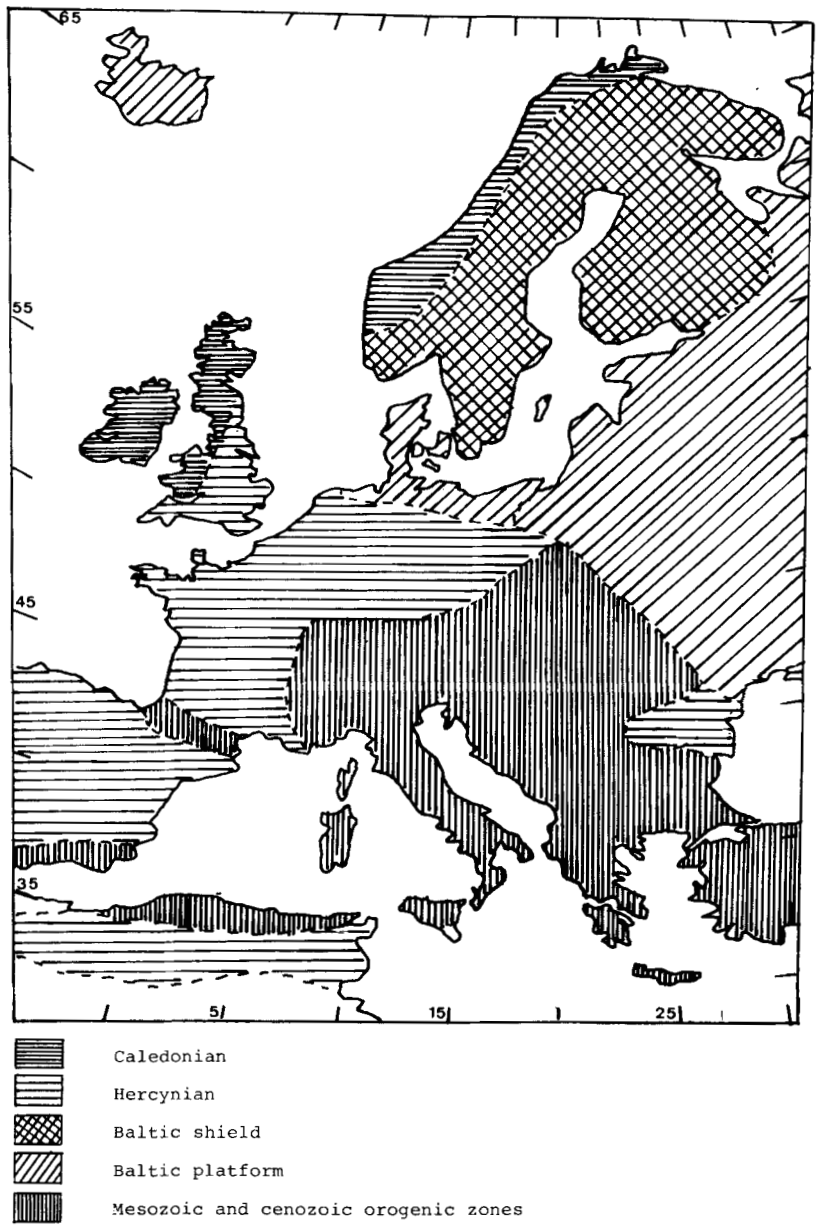

Figure 1. Main tectonic units of western Europe. Adapted from Schatsky *et al.* (1964).

selection of stations and events proceeded in the same way as described in Paper I. Events were kept of magnitude m_b greater than 5.5, with standard errors on latitude and longitude less than 0.05°, and observed by at least 20 stations in western Europe. A total of 1157 events and 114 stations were kept.

Fig. 2 shows the distribution of source regions obtained: although the azimuthal coverage is satisfactory, it is to be noted that the sampling of epicentral distances is poorer than for the United States, a majority of events corresponding to an epicentral distance greater than 50°. Relative travel time residuals (see Paper I) were calculated with respect to the conti-

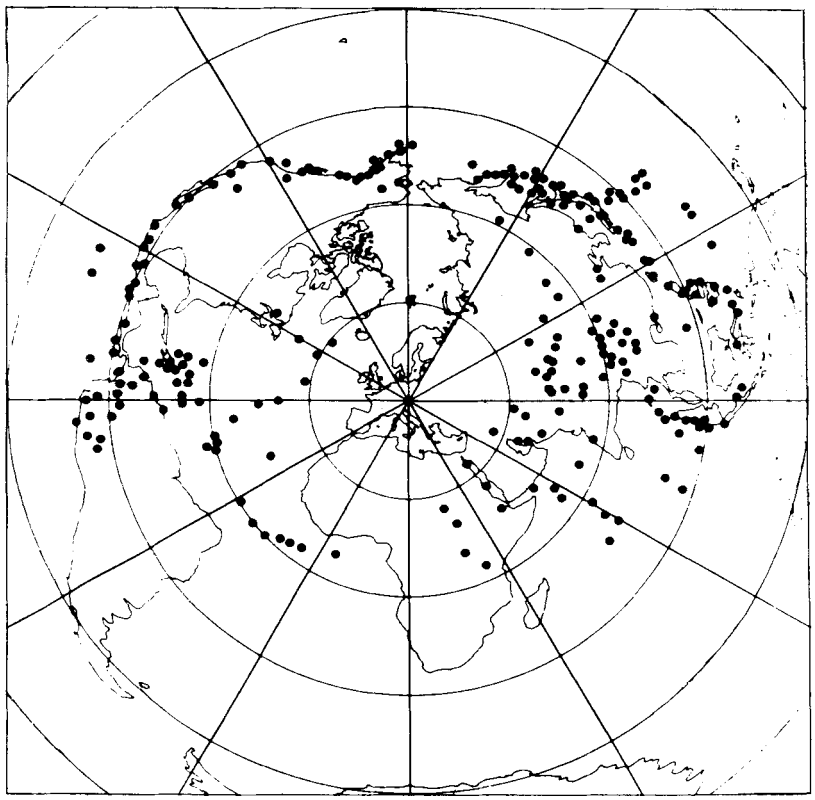

Figure 2. Distribution of source regions for the events used in this study.

nental PEM velocity model (Dziewonski, Hales & Lapwood 1975), which was here chosen because of the smaller bias in residuals versus epicentral distance as compared to the classical Jeffreys–Bullen tables (Jeffreys & Bullen 1940). Corrections for ellipticity and station elevations were applied. Fig. 3 gives the location of stations used and the distribution of station anomalies, defined as averages, for each station, of relative anomalies over all events recorded. The values of these station anomalies are tabulated in Table 1, together with the number of events used in calculating them and the standard deviations of the mean. These station anomalies are in good agreement with previous studies (Herrin & Taggart 1968; Lilwall & Douglas 1970; Poupinet 1978) and illustrate the distinction between the Scandinavian shield (strongly negative residuals < -0.5 s) and the rest of the area, characterized by mildly to strong positive value. Such station anomalies are usually representative of upper mantle structure beneath the stations (Cleary & Hales 1966). Note the exceptionally strong negative anomaly in northern Italy (TRI) and the negative anomalies in Greece; the latter have been previously observed and explained in terms of the presence of a subduction slab in this region of the Aegean Arc (Gregersen 1977).

The inversion method

In order to infer velocity anomalies in the upper mantle from travel-time residuals, the same three-dimensional method was used as in Paper I, to which we refer the reader for detailed description and discussion. The method is derived from the original inversion method of Aki, Christoffersson & Husebye (1976; 1977).

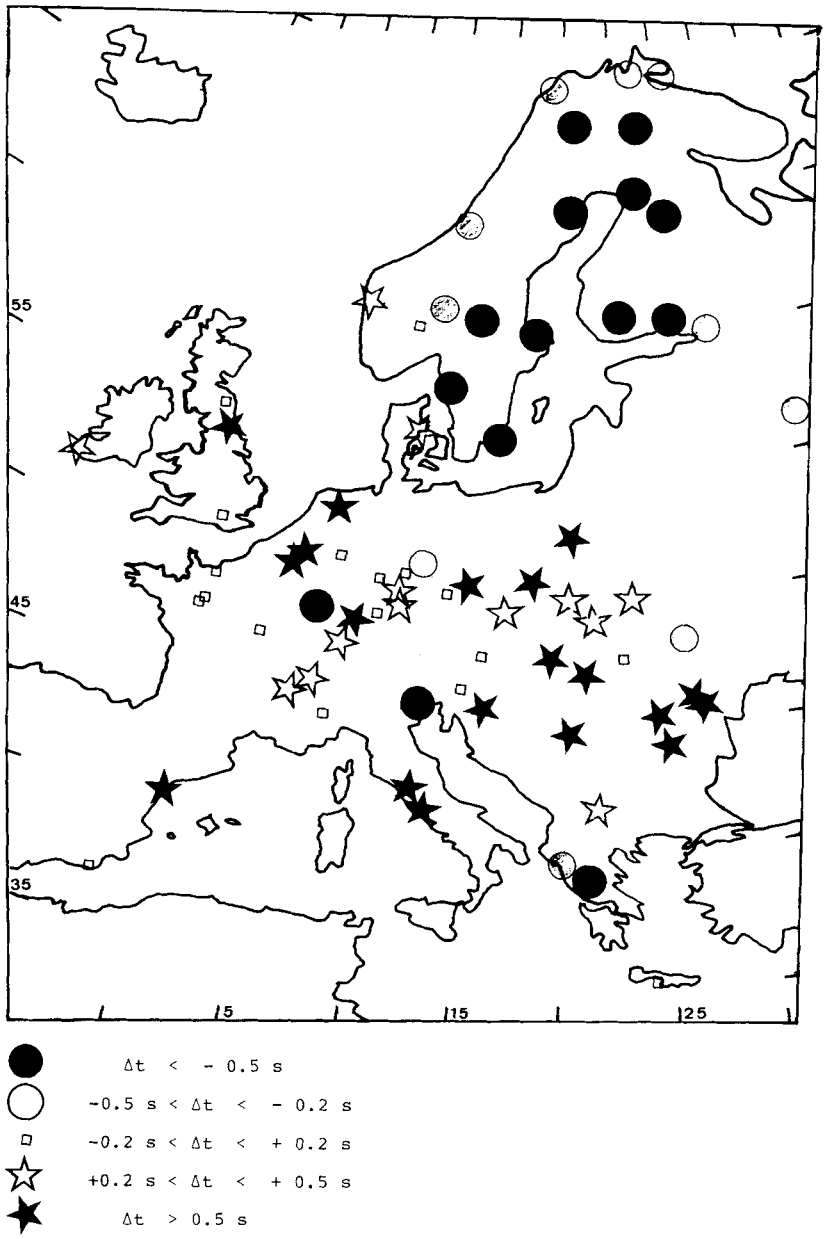

Figure 3. Distribution of stations and relative *P* station anomalies (labelled Δt).

The upper mantle is investigated to a depth of 700 km, and the volume of the Earth thus determined under the stations is divided into three-dimensional blocks (see Paper I). The lateral size of blocks is determined essentially by the station distribution: in spite of a concentration of stations in central Europe on the one hand, in Scandinavia, on the other, some important gaps, in particular in the transition region from stable Precambrian to younger provinces (Fig. 3), limit us to considering $4^\circ \times 4^\circ$ or $5^\circ \times 5^\circ$ blocks. With such a block size, it is possible to distinguish three layers, each 200–250 km thick, which we chose to coincide

Table 1. Relative *P* station anomalies over western Europe given in seconds, with the number of events used to calculate them and the corresponding standard deviation of the mean.

Station	Δt_{sec}	N	σ	Station	Δt_{sec}	N	σ	Station	Δt_{sec}	N	σ
ALI	0.63	226	0.11	LHN	−0.24	379	0.04	UPP	−0.82	1082	0.02
ALM	−0.16	209	0.10	LIS	0.76	232	0.11	UZH	0.35	821	0.04
AQU	0.20	277	0.11	LJU	−0.23	869	0.03	VAL	0.39	608	0.04
ATH	−0.84	694	0.05	LNS	−0.06	630	0.04	VAM	−0.29	431	0.08
ATU	−1.10	27	0.18	LOR	−0.29	912	0.02	VIE	0.27	633	0.04
BAC	0.60	361	0.08	LVV	0.36	569	0.04	VLS	−0.60	467	0.05
BAS	0.26	335	0.09	MAL	−0.00	147	0.12	VRI	0.53	411	0.06
BDB	−0.41	241	0.08	MES	−0.07	201	0.14	VYB	−0.87	93	0.12
BER	0.45	702	0.04	MNY	0.04	508	0.05	WAR	0.66	69	0.17
BES	−0.01	506	0.05	MOS	−0.10	872	0.04	WIT	1.11	801	0.03
BNS	0.03	954	0.02	MOX	−0.14	1061	0.02	WLS	−0.75	504	0.10
BOL	1.48	62	0.25	MSS	0.14	9	0.25	ZAG	0.62	444	0.08
BRA	−0.01	755	0.06	NIE	0.42	714	0.03				
BUC	0.65	498	0.07	NPL	1.10	53	0.27				
BUD	0.63	358	0.07	NUR	−0.51	1073	0.02				
CFF	0.59	155	0.10	OUL	−0.83	503	0.04				
CHZ	0.67	45	0.14	PAD	2.00	158	0.17				
CLL	−0.25	1044	0.02	PAT	0.39	45	0.25				
CMP	1.06	661	0.06	PAV	0.54	136	0.19				
COP	0.47	869	0.04	PRA	0.48	770	0.04				
CRT	0.56	93	0.18	PRU	0.11	1059	0.02				
DEB	1.72	16	0.59	PRT	0.05	13	0.62				
DOU	0.54	887	0.05	PTO	−0.48	55	0.36				
DUR	0.61	603	0.07	PUL	−0.19	809	0.03				
EBR	0.29	473	0.07	PSZ	0.11	125	0.15				
EKA	0.01	827	0.03	RAC	0.92	146	0.11				
FEL	−0.40	78	0.10	RAV	−0.03	39	0.17				
FLN	−0.06	825	0.03	PRK	0.01	480	0.05				
FOC	1.30	235	0.12	RBN	1.85	5	0.70				
FUR	0.13	745	0.03	RCI	1.05	63	0.26				
GOT	−0.59	224	0.07	ROM	0.38	358	0.08				
GRF	0.36	577	0.03	RSL	−0.13	618	0.04				
GRC	−0.17	462	0.03	SAR	1.32	16	0.56				
GRR	−0.08	816	0.03	SKA	−0.50	288	0.05				
HEI	−0.14	62	0.09	SIM	0.10	785	0.04				
HLE	−0.25	156	0.08	SOC	−0.01	414	0.05				
IAS	−0.05	514	0.06	SOD	−0.53	1082	0.03				
ISO	−0.11	515	0.05	SOF	0.30	364	0.08				
JEN	0.01	139	0.11	SOP	−0.17	181	0.12				
KEV	−0.16	1018	0.03	SSC	−0.17	843	0.03				
KEW	0.07	317	0.05	SSF	−0.04	849	0.03				
KHC	−0.01	1043	0.02	STR	0.49	846	0.04				
KJN	−0.53	837	0.03	STU	−0.26	786	0.03				
KIR	−0.65	1063	0.02	TOL	−0.52	82	0.35				
KIS	−0.24	710	0.04	TRI	−1.17	612	0.02				
KIP	0.63	20	0.59	TRO	−0.21	949	0.03				
KLS	−0.90	242	0.06	TRS	−0.05	14	0.27				
KON	0.07	932	0.03	TUB	0.36	18	0.17				
KRA	0.21	951	0.03	UCC	0.84	580	0.06				
KRK	0.03	469	0.04	UDD	−0.85	143	0.10				
KRL	−1.12	11	0.83	UME	−0.87	1031	0.03				

in depth with those of Paper I (layer 1: 0–250 km; layer 2: 250–450 km; layer 3: 450–700 km). The initial velocity model is PEM-C (Dziewonski *et al.* 1975), the same as for the calculation of the travel-time residuals. Before the inversion, and in order to eliminate short-wavelength features associated with the sources, the data were averaged over 4° x 4° source regions, yielding 15021 'average rays' to be used as input data for the inversion (see Paper I). The inversion was performed using a generalized inverse technique with eigenvector and eigenvalue decomposition and a cut-off criterion for the smallest eigenvalue (Lanczos 1961; Wiggins 1972). As discussed in Paper I, it is found here too that a cut-off value for the eigenvalues of about $\lambda_{max}/\lambda_{min} = 5 \times 10^2$ is optimal. With the method used, solutions yield only relative velocity anomalies with respect to the average velocity in each layer.

The average velocity in each layer remains undefined and, consequently, we can only discuss the relative variation of velocity anomalies across a layer, not their absolute values. A difference with the smaller scale, flat Earth models (Aki *et al.* 1976) comes from the fact that rays originating at a given source do not spend exactly the same time in a given layer, thus replacing a number of zero eigenvalues by small but not strictly zero eigenvalues.

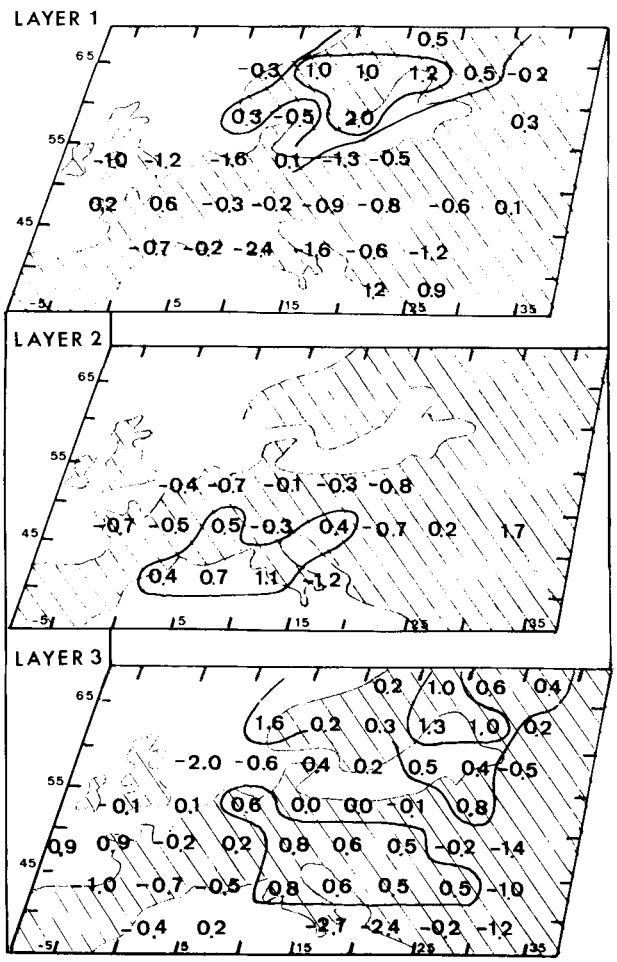

Figure 4. Results of a three-layer inversion with 5° x 5° blocks (layer 1: 0–250 km; layer 2: 250–450 km; layer 3: 450–700 km). Velocity anomalies in each layer are expressed in percentage of average velocity in the layer. Contours emphasize regions of positive velocity anomalies.

Table 2. Diagonal elements of the resolution matrix for the model presented in Fig. 4. The lower left hand side corner in each layer, corresponds to latitude 35° N and longitude + 10° W.

Layer 1

–	–	–	–	–	0.87	0.93	0.94	0.90	–
					(96)	(180)	(345)	(50)	
–	–	0.73	0.94	0.95	0.96	0.96	0.95	0.94	–
		(53)	(152)	(349)	(155)	(239)	(417)	(60)	
–	0.90	0.64	0.93	0.96	0.97	0.00	0.86	0.91	0.82
	(222)	(15)	(75)	(405)	(224)	(3)	(36)	(84)	(146)
–	0.95	0.97	0.97	0.98	0.98	0.97	0.12	–	–
	(177)	(271)	(501)	(821)	(277)	(193)	(7)		
–	0.97	0.97	0.97	0.98	0.98	0.97	0.97	0.94	0.82
	(375)	(845)	(1405)	(1019)	(928)	(617)	(756)	(93)	(17)
–	0.69	0.94	0.97	0.97	0.97	0.97	0.97	0.87	0.84
	(84)	(196)	(225)	(338)	(41)	(164)	(162)	(57)	(85)
0.85	0.89	0.72	–	0.68	0.85	0.91	0.94	–	–
(63)	(320)	(39)		(16)	(151)	(484)	(137)		

Layer 2

–	–	–	–	0.59	0.71	0.82	0.86	0.86	0.18
				(34)	(91)	(256)	(195)	(196)	(13)
–	–	0.29	0.80	0.88	0.90	0.93	0.90	0.89	0.00
		(49)	(180)	(226)	(223)	(218)	(232)	(204)	(1)
0.41	0.77	0.81	0.86	0.90	0.89	0.85	0.63	0.76	0.51
(27)	(155)	(77)	(84)	(304)	(185)	(65)	(47)	(78)	(121)
0.17	0.89	0.94	0.95	0.95	0.96	0.94	0.88	0.00	0.33
(15)	(154)	(314)	(587)	(699)	(448)	(302)	(68)	(2)	(24)
–	0.92	0.94	0.95	0.95	0.95	0.95	0.93	0.92	0.82
	(244)	(898)	(1283)	(973)	(921)	(548)	(641)	(214)	(83)
0.03	0.39	0.91	0.94	0.95	0.95	0.92	0.91	0.77	0.50
(6)	(105)	(219)	(157)	(268)	(123)	(143)	(199)	(22)	(98)
0.61	0.75	0.67	0.00	0.36	0.71	0.78	0.77	0.00	–
(104)	(252)	(70)	(1)	(30)	(157)	(325)	(225)	(1)	

Layer 3

–	–	–	0.55	0.81	0.93	0.92	0.92	0.92	0.92
			(16)	(84)	(100)	(118)	(155)	(217)	(114)
–	0.05	0.87	0.94	0.96	0.96	0.96	0.95	0.95	0.95
	(7)	(59)	(143)	(197)	(206)	(108)	(184)	(186)	(113)
0.82	0.89	0.93	0.97	0.97	0.97	0.97	0.94	0.94	0.93
(56)	(88)	(151)	(146)	(129)	(222)	(113)	(61)	(75)	(137)
0.84	0.95	0.97	0.98	0.98	0.98	0.98	0.98	0.90	0.61
(58)	(136)	(474)	(602)	(699)	(680)	(388)	(167)	(21)	(30)
0.96	0.96	0.97	0.98	0.98	0.98	0.98	0.97	0.97	0.94
(52)	(238)	(674)	(915)	(895)	(705)	(562)	(477)	(371)	(159)
0.90	0.95	0.97	0.97	0.98	0.97	0.97	0.96	0.96	0.80
(37)	(139)	(273)	(168)	(210)	(227)	(206)	(226)	(92)	(68)
0.83	0.87	0.92	0.95	0.76	0.96	0.96	0.95	0.95	0.72
(121)	(154)	(87)	(22)	(30)	(111)	(155)	(218)	(45)	(7)

Because of the cut-off criterion used, this is reflected in the solutions by introducing non-strictly zero average velocity anomalies in each layer, and these can also vary from one solution to another. This, however, does not impede our discussion of relative trends of the aomalies.

Presentation of results

We have chosen to present results for several inversions, shown in Figs 4, 5 and 6, in order to be able to judge the stability of the models obtained with respect to changes in the initial model specifications and the possible influence of heterogeneities outside the volume sampled by the blocks. The velocity anomalies are, in each case, expressed as a percentage of average velocity in the layer, and only those values are shown, which correspond to blocks with resolution greater than 0.90.

Fig. 4 presents the result of an inversion with three layers of $5^\circ \times 5^\circ$ blocks in each layer. The diagonal elements of the resolution matrix for this model are listed in Table 2, with the number of rays sampling each block. As can be seen from Table 2, while layers 1 and 3 are well resolved, only a small number of blocks can be considered as resolved in layer 2 (blocks with resolution less than 0.9 are usually poorly constrained). This is true for all three solutions shown, and comes mainly from the fact that the data sample a narrow epicentral distance band, as mentioned earlier, which corresponds, in most azimuths, to epicentral distances greater than 50°. Most of the rays are therefore very steep to depths of 300 to 400 km from the stations, and an insufficient cross-sampling of rays is achieved in layer 2.

The scatter in the European travel-time anomalies (by which we understand the standard deviation calculated on the travel-time anomalies for all stations and all events) is much larger than for the United States ($\sigma_d = 1.5$ s compared to 0.9 s for the United States). This can be due to the large-amplitude short-wavelength variations of structure, as mentioned earlier (Souriau 1978). The $5^\circ \times 5^\circ$ blocks are not well suited to reflect small-scale variations, and can only yield very smoothed long-wavelength features. This point is well expressed in the fact that, in terms of reduction of standard deviation in travel-time residuals, our models explain 33 per cent of the data, which is somewhat less than for the US (Romanowicz 1979). Therefore, as usual with this type of method, one should not attach too much importance to the actual velocity anomalies obtained, but rather to their trends and the regionalization they determine, if the latter is conserved from one model to another. Table 3 shows the standard deviations of the model parameters corresponding to the model presented in Fig. 4. These standard deviations are calculated assuming a standard deviation of 1 s, in the data, estimated from the fraction of travel-time anomalies not explained by the model (Aki *et al.* 1976). Table 3 confirms the result that we cannot attach significance to the results of layer 2.

Fig. 5 shows the results obtained by considering the same layers as in Fig. 4, $5^\circ \times 5^\circ$ blocks in the two deepest layers, and $4^\circ \times 4^\circ$ blocks in the first layer. Compared to the solution shown in Fig. 4, this one shows lateral variations of larger amplitude in the first layer, where blocks are smaller, it is therefore less smooth, while it manages to explain only a little more of the data (34 per cent in terms of standard deviation in the residuals). However, the trends and regionalization of anomalies remain stable. We have therefore continued to perform inversions using larger blocks, preferring smoother solutions that give a clearer idea of the large-scale trends we are interested in.

As it is somewhat arbitrary to limit the region studied to a depth of 700 km, as discussed in Paper I, and assume that the rest of the mantle is homogeneous for the bundle of rays originating at a given source, it may well be that some deeper heterogeneities are taken up by the models. In order to somewhat clarify this point, an inversion with $5^\circ \times 5^\circ$ blocks was performed, introducing into the equations an additional term expressing the dependence of the residual on epicentral distance. For each 'ray', the corresponding equation is here:

$$\Delta t_{ij}^r = \sum_k a_k^{ij} x_k + f_{ij}(\Delta)$$

Table 3. Standard errors for the model presented in Fig. 4 expressed in percentage of average velocity in each layer. Blocks are represented in the same arrangement as in Fig. 4, the lower left hand side limit, for each layer, corresponding to latitude 35° N and longitude +10° W.

Layer 1

-	-	-	-	-	0.56	0.38	0.28	0.48	-
-	-	0.42	0.40	0.26	0.34	0.26	0.24	0.44	-
-	0.36	0.60	0.42	0.26	0.28	0.08	0.58	0.44	0.46
-	0.32	0.26	0.24	0.20	0.24	0.34	1.08	-	0.76
-	0.30	0.22	0.28	0.28	0.30	0.22	0.24	0.38	0.70
-	0.64	0.34	0.26	0.28	0.48	0.34	0.30	0.44	0.44
1.00	0.34	0.60	-	0.64	0.48	0.38	0.36	-	-

Layer 2

-	-	-	-	0.62	0.66	0.54	0.44	0.42	0.74
-	-	0.38	0.62	0.44	0.46	0.44	0.42	0.48	0.04
0.60	0.48	0.56	0.60	0.46	0.43	0.64	0.72	0.60	0.68
0.58	0.54	0.40	0.32	0.30	0.34	0.44	0.62	0.10	0.66
-	0.50	0.34	0.26	0.26	0.28	0.32	0.36	0.44	0.54
0.26	0.76	0.50	0.44	0.44	0.50	0.48	0.42	0.78	0.52
0.46	0.44	0.60	0.04	0.46	0.64	0.46	0.50	0.06	-

Layer 3

-	-	-	0.74	0.54	0.38	0.42	0.36	0.34	0.40
-	0.60	0.52	0.50	0.36	0.32	0.32	0.32	0.32	0.36
0.50	0.48	0.40	0.34	0.38	0.34	0.36	0.46	0.42	0.40
0.54	0.44	0.26	0.24	0.20	0.24	0.23	0.32	0.62	0.72
0.46	0.28	0.22	0.20	0.18	0.20	0.20	0.24	0.28	0.38
0.58	0.36	0.28	0.28	0.28	0.30	0.28	0.32	0.36	0.58
0.48	0.44	0.46	0.58	0.72	0.44	0.36	0.38	0.46	0.80

where Δt_{ij}^{r} is the relative travel-time residual for ray ij, x_k are the unknown relative velocity anomalies in each block k, a_k^{ij} are matrix element functions of the initial model and ray paths, and $f_{ij}(\Delta)$ is an unknown function of epicentral distance from the source j to the station i. We took 5° steps in epicentral distance to define the function $f(\Delta)$. The function f should absorb any systematic variation of the travel-time residuals observed with epicentral distance, and the upper mantle model should not be significantly affected by this new formulation. The results are shown in Fig. 6, for the upper mantle, while the function f is depicted in Fig. 7. As can be seen from Figs 6 and 7, the main features of the solution are conserved, and the function f reflects the worldwide trend of travel-time anomalies for P waves with the characteristic minimum around 60 of epicentral distance (this minimum is present in the PEM model, but has a smaller amplitude than in the Jeffreys–Bullen model; Dziewonski *et al.* 1975). This model explains only insignificantly more of the scatter in the data than the previous models (34 per cent), which, together with the stability of the main features in the velocity trends, shows that the block geometry does not absorb a significant part of lower mantle inadequacies of the initial velocity model.

The models presented here, although not identical, show striking large-scale common

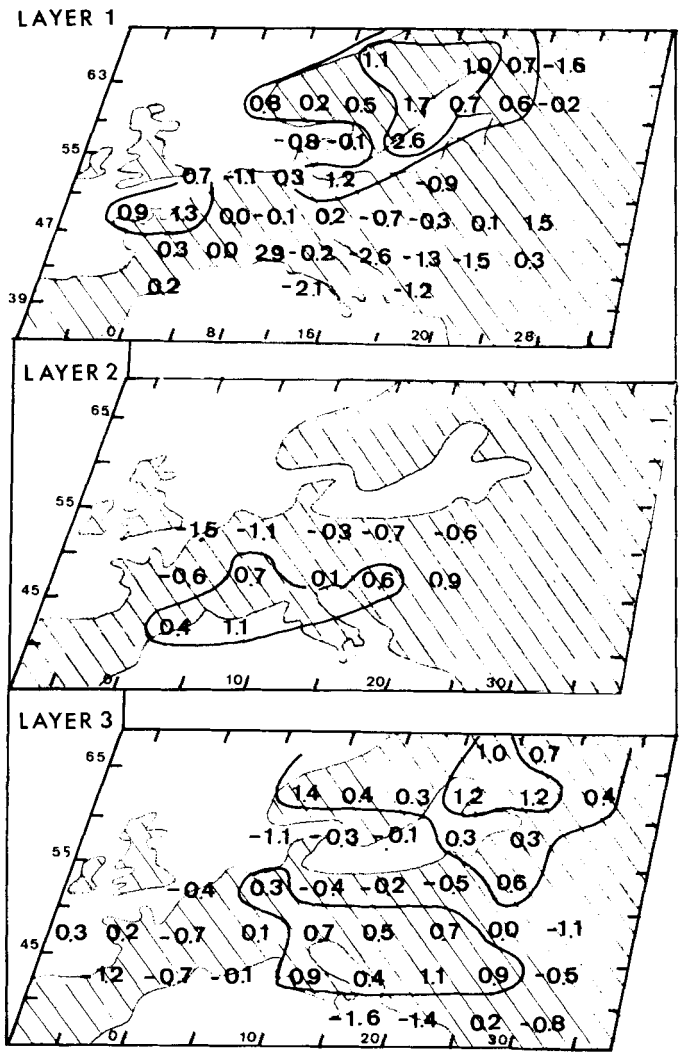

Figure 5. Results of a three-layer inversion with the same layers as in Fig. 4, 4° × 4° blocks in the first layer, 5° × 5° blocks in the second and third layers.

features, which we shall now discuss layer by layer. Their validity will be assessed by comparison with independent studies of the structure of Europe.

Discussion

Models for layer 1 give velocity fluctuations averaged over the first 250 km of the mantle. It is therefore impossible to distinguish between contributions of the crust, Moho, or deeper mantle heterogeneities, such as a possible low velocity zone. A comparison with other models giving velocity–depth curves is therefore very useful. Results show that the average *P* wave velocity in the depth range 0–250 km is up to 4 per cent higher in the region of Scandinavia than in southern Europe, where it reaches a minimum under the Alps of northern Italy and the northern Adriatic. This is in agreement with previous studies of *P* velocity in Europe (King & Calcagnile 1976; England & Worthington 1976; England *et al.*

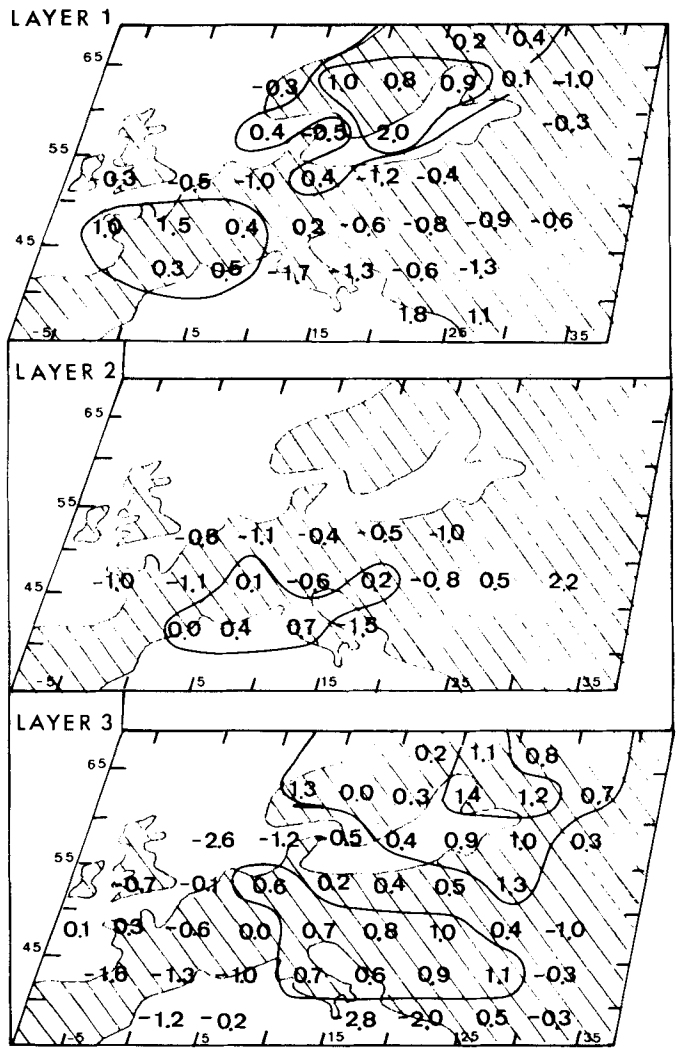

Figure 6. Results of a three-layer inversion using 5° × 5° blocks and the same layers as in Figs 4 and 5, taking into account the average variation of travel-time residuals with epicentral distance.

1978), which show higher average velocities under the shield and platform than under south-western Europe, due to the existence, in the latter region, of a mantle low-velocity zone, that is not required by the data for the stable parts. The results are also easily reconcilable with surface-wave studies (Knopoff *et al.* 1966; Nolet 1978; Cara *et al.* 1980), if one associates the *P* low-velocity zone with the *S* low-velocity zone, as proposed by Mayer-Rosa & Mueller (1973) for southern Europe. The *P* low-velocity zone would thus also be maximally developed in the Alps.

Some smaller scale observations can also be tentatively made for this layer: velocities under the Scandinavian Shield increase from the ocean inland, in agreement with the slowness anomaly study by Noponen (1974). In addition, average velocity under part of France, corresponding roughly to the Hercynian Britanny area, and east of it, appears to be higher than elsewhere in southern Europe, which can be explained by a thinning of the low-velocity zone; this is in agreement with a small-scale surface-wave study the subject of which was to

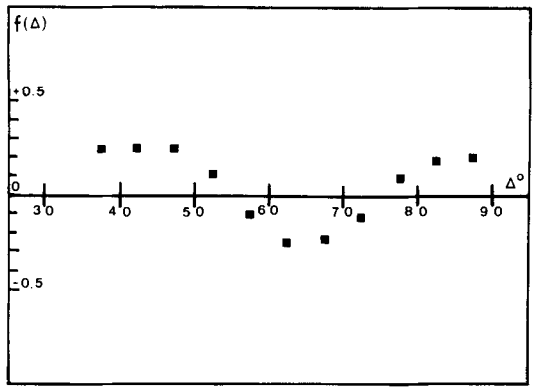

Figure 7. Variations of the function $f(\Delta)$ (in seconds) as a function of epicentral distance. This function represents the common trend of the travel-time residuals obtained simultaneously with the upper mantle model presented in Fig. 6.

compare the lithosphere in Hercynian France with that in the Baltic Shield (Souriau 1978): models for these two regions differ only by the values of velocities in the lid, higher by 3 per cent in the shield (*S* wave velocities). To the north of this zone of relatively high velocities, a region of rather strong slow anomalies covers Great Britain, again in agreement with local surface-wave studies, showing a well-developed low-velocity zone under western England and Ireland (Jacob 1969). The higher velocities found under Greece reflect the negative station anomalies observed in this region, but the spatial spread may only be an artifact of the sampling by large blocks, which happen to be situated, in addition, on the edge of the model, and are thus less well constrained.

Layer 2 (250–450 km) is unfortunately not very well resolved, which does not allow a detailed discussion. It seems however, that a region of higher velocities exists in southern Europe, and that these velocities decrease towards the north and west. The velocity anomalies in this layer are not much in excess of 1 per cent. Although, due to poor resolution, possible numerical effects cannot be discarded, these results would be comparable to the situation found in North America, where, in this depth range, velocities are lowest in the central stable part, increasing under the Appalachians and the Cordilleran belt.

In layer 3, velocity anomalies are better resolved than in layer 2 due to a better cross-sampling by rays that are significantly inclined with respect to the vertical. Velocity contrasts average ± 1.5 per cent, which is somewhat less than found at this depth in the United States (Paper I). A broad region of relatively high velocities covers the Baltic Shield, where velocities are highest under Finland. Velocities decrease towards the west and particularly the south-west, in the direction of the Hercynian parts and the ocean. The high velocities under the shield and platform can be compared with those found under the central United States, in the same depth range, suggesting that this may be a characteristic feature of deep upper mantle structure under shields. It may be an indication of the existence of deep continental roots, as proposed by Jordan (1978). Since the major structural feature at these depths is the well known 650 km discontinuity in seismic velocities, another possible interpretation, although totally speculative, is in terms of variations in depth of this discontinuity, caused for example by lateral temperature variations in the mantle (Romanowicz 1979). Before more credit can be given to such a speculative interpretation, more evidence for upper mantle discontinuities has of course to be found independently.

The features in the deep velocity variations described above are the most prominent

common features of all the solutions. Under the Alps and the Adriatic region, the velocities seen to increase again, but the amplitudes of the anomalies are only half as large as those under the shield, and this area is separated from the latter only by a narrow band of mild velocity minima, which may not be significant. It can thus be said that the velocity anomalies under central Europe and the Alps, in the depth range from 450 to 700 km, are not particularly marked. It is interesting to compare this again with the results obtained for the western United States, where, in this layer, velocities decrease steadily from east to west, as one moves from the central stable plains to the tectonically young mountain belt. The difference in trends may be viewed in terms of the distinct modes of formation of these two mountain belts, and suggests the speculation whereby the continent–continent collision involved in the formation of the Alps could still be inprinted in the deep structure of this region, as has already been suggested by England *et al.* (1976), who called anomalous the structure under southern Europe between depths of 300 and 500 km.

Conclusions

The present study of upper mantle *P* velocity fluctuations under western Europe shows significant large-scale lateral variations of structure to depths of at least 700 km. The models manage to explain only one third of the scatter in the data, suggesting that smaller scale variations are, as one would expect, dominant in Europe. The trends of the large-scale fluctuations and their geographical distribution are, however, stable from one solution to another, and agree with previous studies of upper mantle structure in Europe where such studies exist, in the upper 250 km of the mantle. We therefore feel we can attach some confidence to our results for the deeper part of the upper mantle as well as for the first layer, until some independent study of this deeper part can confirm or contradict them.

In the first 250 km of the mantle, velocities are highest under the Baltic Shield and lowest under the Alps, in agreement with previous studies and with the view that young tectonic provinces have well-developed mantle low-velocity zones, while Precambrian shields have none or very weak ones. In the depth range 250–450 km, not much can be said, due to the poor resolution of the models. Between 450 and 700 km depth, velocities are again highest under the shield, decrease towards the Atlantic, but are rather mild under the Alps, which, compared with results obtained in the western United States, suggests that the mode of formation of orogenic belts may play an important role in the present structure down to depths of several hundreds of kilometres. It remains to be seen whether these structural features appear as a cause or a consequence of the tectonic processes. High velocities under shields and platforms are depths of the order of 500–600 km may well represent a general feature, as they are observed under North America and Europe equally.

Acknowledgments

The author wishes to thank the anonymous reviewer and Dr Dewey for their comments which have contributed to improving this paper.

This paper is Contribution IPGP No. 375.

References

Aki, K., Christoffersson, N. & Husebye, E., 1976. Three dimensional seismic structure of the lithosphere under Montana, LASA, *Bull. seism. Soc. Am.*, 68, 501–524.

Aki, K., Christoffersson, N. & Husebye, E., 1977. Determination of the three dimensional seismic structure of the lithosphere, *J. geophys. Res.*, 82, 277–296.

Cara, M., Nercessian, A. & Nolet, G., 1980. New inferences from higher mode data in Western Europe and Northern Eurasia, *Geophys. J. R. astr. Soc.*, **61**, 459–478.

Cleary, J. & Hales, A., 1966. An analysis of the travel times of *P* waves to North American stations in the distance range 32° to 100°, *Bull. seism. Soc. Am.*, **56**, 467–489.

Dziewonski, A. M., Hales, A. & Lapwood, F., 1975. Parametrically simple Earth models consistent with geophysical data, *Phys. Earth planet. Interiors*, **10**, 12–48.

England, P. C., Kennett, B. L. N. & Worthington, M. H., 1978. A comparison of the upper mantle structure beneath Eurasia and the North Atlantic and Arctic Oceans, *Geophys. J. R. astr. Soc.*, **54**, 575–585.

England, P. C. & Worthington, M. H., 1976. The travel times of *P* seismic waves in Europe and Western Russia, *Geophys. J. R. astr. Soc.*, **48**, 63–70.

England, P. C., Worthington, M. H. & King, D. W., 1976. Lateral variation in structure of the upper mantle beneath Eurasia, *Geophys. J. R. astr. Soc.*, **48**, 71–79.

Gregersen, S., 1977. *P* wave travel time residuals caused by a dipping plate in the Agean Arc in Greece, *Tectonophysics*, **37**, 83–94.

Herrin, E. & Taggart, J., 1968. Regional variations in *P* travel times, *Bull. seism. Soc. Am.*, **58**, 1325–1337.

Jacob, A. W. B., 1969. Crustal and upper mantle structure in Ireland and the south of Scotland, *thesis*, University of Dublin.

Jeffreys, H. & Bullen, K., 1940. *Seismological Tables*, British Association for the Advancement of Science.

Jordan, T. H., 1978. Composition and development of the continental Tectonosphere, *Nature*, **274**, 544–548.

King, D. W. & Calcagnile, G., 1976. *P* wave velocities in the upper mantle beneath Fennoscandia and western Russia, *Geophys. J. R. astr. Soc.*, **46**, 407–432.

Knopoff, L., Mueller, S. & Pilant, W. L., 1966. Structure of the crust and upper mantle in the Alps from the phase velocity of Rayleigh waves, *Bull. seism. Soc. Am.*, **56**, 1009–1044.

Lanczos, C., 1961. *Linear Differential Operators*, D. Van Nostrand, London.

Lilwall, R. C. & Douglas, A., 1970. Estimation of *P* wave travel times using the joint epicenter method, *Geophys. J. R. astr. Soc.*, **19**, 165–181.

Mayer-Rosa, D. & Muller, St., 1973. The gross velocity–depth distribution of *P* and *S* waves in the upper mantle of Europe from earthquake observations, *Z. Geophys.*, **39**, 395–410.

McKenzie, D., 1972. Active tectonics of the Mediterranean region, *Geophys. J. R. astr. Soc.*, **30**, 109–186.

Nolet, G., 1977. The upper mantle under Western Europe inferred from the dispersion of Rayleigh waves, *J. Geophys.*, **43**, 265–285.

Noponen, I., 1974. Seismic ray direction anomalies caused by deep structure in Fennoscandia, *Bull. seism. Soc. Am.*, **64**, 1931–1941.

Patton, H. J., 1978. Source and propagation effects of Rayleigh waves from central Asian earthquakes, *PhD thesis*, M.I.T., Cambridge, Mass.

Poupinet, G., 1977. Hétérogénéités du manteau terrestre déduites de la propagation des ondes de volume-implication géodynamique, *Thèse d'Etat*, Grenoble, France.

Prodehl, C., 1977. The structure of the crust mantle boundary beneath North America and Europe as derived from explosion Seismology, in *The Earth's Crust*, ed. Heacock, T. G., *A.G.U. Monograph 20*.

Panza, G. F., 1978. The gross feature of the lithosphere–asthenosphere system in t e European Mediterranean area, *E.G.S. Meeting*, Strasbourg.

Romanowicz, B., 1979. Seismic structure of the upper mantle beneath the United States by three dimensional inversion of body wave arrival times, *Geophys. J. R. astr. Soc.*, **57**, 479–506.

Romanowicz, B. & Allègre, C. J., 1979. Deep structure of the continents: possible topography of the upper mantle phase change discontinuities, *EOS Trans. Am. Geophys. Un.*, **60**, 397.

Schatsky, N. S., Bogdanoff, A. A. & Mouratov, M. V., 1964. *Tectonics of Europe, International geological congress*, Nauka, Moscow.

Seidl, D., 1971. Spezielle Probleme der Ausbreitung seismischen Oberflächwellen mit Beobachtungsbeispielen aus Europa, *PhD thesis*, Karlsruhe.

Sprecher, C., 1976. Die Struktur ds oberen Erdmantels in Zentraleuropa aus Dispersionsmessungen an Rayleighwellen, *PhD thesis*, Zurich.

Souriau, A., 1978. Le Manteau supérieur sous la France et les régions limitrophes du Nord, *Thèse d'Etat*, Université Paris VI.

Tapponnier, P., 1977. Evolution tectonique du système alpin en Méditerranée: poinçonnement et écrasement rigide-plastique, *Bull. Soc. géol. France,* **XIX,** 437–460.

Wiggins, R. A., 1972. The general inverse problem: implications of surface waves and free oscillations for Earth structure, *Rev. Geophys.*, **10,** 251–285.